

Infrared, Raman, and DFT Vibrational Spectroscopic Studies of $C_{60}F_{36}$ and $C_{60}F_{48}$ Alexey A. Popov,^{*,†} Vladimir M. Senyavin,[†] Olga V. Boltalina,^{*,‡,§} Konrad Seppelt,[§] Johann Spandl,[§] Charles S. Feigerle,^{||} and Robert N. Compton^{||}

Chemistry Department, Moscow State University, Leninskie Gory, 119992 Moscow, Russia, Department of Chemistry, Colorado State University, Fort Collins, Colorado 80523, Institute of Inorganic Chemistry, Freie University, Berlin D14195, Germany, and Department of Chemistry, The University of Tennessee, Knoxville, Tennessee 37996

Received: February 1, 2006; In Final Form: April 29, 2006

IR and Raman spectra of two fluorofullerenes, $C_{60}F_{48}$ and $C_{60}F_{36}$, are thoroughly studied. Assignment of the experimental spectra is provided on the basis of density functional theory (DFT) computations. Perfect correspondence between experimental and computed spectra enabled us to confirm that the major isomer of $C_{60}F_{48}$ has D_3 symmetry. It was found that as-synthesized samples of $C_{60}F_{36}$ consist mainly of C_3 and C_1 isomers in ca. 2:1 ratio and 2–3% of T -symmetric structures. Extensive AM1 and DFT computations have shown that all three structures are the most stable isomers of $C_{60}F_{36}$. Previous structural assignment of the C_3 isomer (Gakh, A. A.; Tuinman, A. A. *Tetrahedron Lett.* **2001**, 42, 7137–7139) was confirmed by the vibrational data.

Introduction

In the past decade, considerable progress has been made in the understanding of fluorinated fullerenes.¹ In particular, C_{60} fluorine chemistry has yielded a wealth of new compounds and substitution products which have been shown to exhibit many remarkable physical properties. Among the most recent examples of the latter are the quantum mechanical wave nature of $C_{60}F_{48}$ ² and the ability of highly fluorinated fullerenes (FFs) to considerably increase the conductivity of the diamond surface due to their pronounced electron-accepting properties.³

Despite the current availability of the well-developed synthetic and purification methods for producing some fluorofullerenes^{4–6} along with ongoing interest in these compounds by different research groups, many important properties of these compounds have not yet been determined, including unambiguous structural elucidations for $C_{60}F_{48}$ or redundant proof of the currently accepted (largely on the basis of NMR) structure of the C_3 - $C_{60}F_{36}$ isomer.⁷

$C_{60}F_{48}$ was the first FF selectively synthesized with appreciable yield.⁸ ^{19}F NMR spectroscopy showed the main product molecules (63% by NMR peaks integration) to have eight sets of six fluorine atoms. With the help of 2D COSY spectra, the molecular structure of $C_{60}F_{48}$ was tentatively assigned to the D_3 isomer (Figure 1a), though some anticipated F–F couplings were missing. Another isomer was found as a 10–15% admixture and was assumed to be the S_6 -symmetric *meso* form of the major product (Figure 1b).⁸ While significant improvements have since been made in the preparation techniques, purity, and yields,⁹ the molecular structure of $C_{60}F_{48}$ still retains an ambiguity. Analysis of the single-crystal X-ray data on the $C_{60}F_{48} \cdot 2C_6H_5Me_3$ solvate was complicated by a

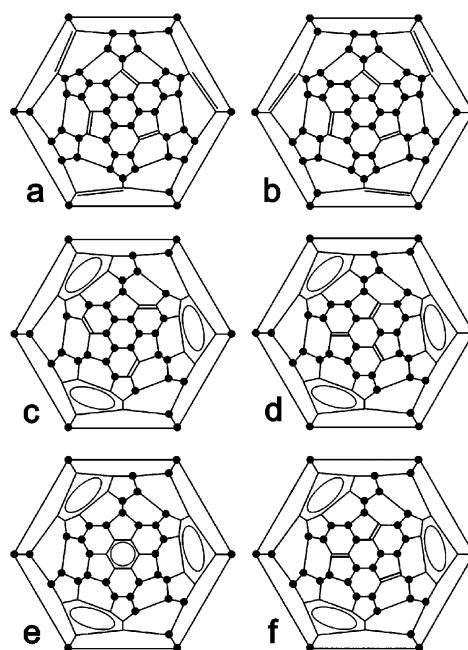


Figure 1. Schlegel diagrams of (a) one enantiomer of D_3 - $C_{60}F_{48}$, (b) S_6 - $C_{60}F_{48}$, (c) $C_3(N3)$ - $C_{60}F_{36}$, (d) $C_3(N64)$ - $C_{60}F_{36}$, (e) T - $C_{60}F_{36}$, and (f) C_1 - $C_{60}F_{36}$.

substantial degree of disorder, leading to concurrent interpretations of 40–70% mixture of the D_3 and S_6 isomers¹⁰ or the S_6 isomer alone.¹¹ Theoretical modeling predicted both structures to be virtually isoenergetic.^{12,13} A recent precise gas-phase electronographic study performed for $C_{60}F_{48}$ under the assumption of the sole presence of either D_3 or S_6 symmetry species showed no difference in the average geometrical parameters between the two structures, thereby precluding conclusions as to the actual gas-phase isomeric composition.¹⁴

Formation of $C_{60}F_{36}$ in the reaction of C_{60} with MnF_3 was first reported in 1995¹⁵ and followed by ^{19}F NMR study which indicated the presence of a mixture of isomers.¹⁶ HPLC

* To whom correspondence should be addressed. E-mail: popov@phys.chem.msu.ru (A.A.P.); ovbolt@lamar.colostate.edu (O.V.B.).

[†] Moscow State University.

[‡] Colorado State University.

[§] Freie University Berlin.

^{||} The University of Tennessee.

separation of the two major isomers revealed that the most abundant isomer had C_3 symmetry, while the other belonged to T symmetry group (Figure 1e). A third isomer, of C_1 symmetry (Figure 1f), which was found to rearrange into more stable C_3 isomer over time, was also isolated and characterized by X-ray diffraction.^{17a}

The proposed structure of the T isomer was confirmed by the X-ray method,^{17b} while the original assignment of the C_3 isomer to a particular structure (Figure 1c) proved to be incorrect; subsequent detailed 1D and 2D ^{19}F NMR analysis allowed the authors to conclude that the other C_3 isomer (shown in Figure 1d), which was also calculated to be the most stable of all C_3 structures, is the most likely structure for the experimentally studied abundant product of the MnF_3 reaction of C_{60} .⁷

Due to the unique sensitivity of vibrational (IR and Raman) spectroscopy to molecular structure, its application can assist substantially in structure elucidation, especially when other commonly used direct methods of structural analysis have failed to provide unambiguous answers. Nevertheless, until very recently, application of vibrational spectroscopy in the fullerene chemistry was very limited; it suffered from the lack of theoretical background, since the required first-principle vibrational calculations were hardly feasible for molecules of such large size ($n(\text{C}) > 60$). Reported examples included mainly vibrational analysis of the parent fullerenes C_{60} ,^{18,19} C_{70} ,²⁰ and C_{84} ,²¹ azafullerene,²² some endohedral metallofullerenes,^{23–26} C_{60} polymers,^{27–32} and four exohedral derivatives, $\text{C}_{60}\text{Br}_{24}$,³³ $\text{C}_{60}\text{F}_{20}$,³⁴ C_{60}Cl_6 ,³⁵ and $\text{C}_{60}\text{Cl}_{30}$.³⁶ The B3LYP/6-31G* approach was successfully used to provide complete assignment of C_{60} and C_{70} vibrational spectra with reported deviations from experimental data of less than 5 cm^{-1} .^{18,20} Computations of the IR spectra of two C_{84} isomers at this level of theory have also shown qualitative agreement with experimental data.²¹ However, first principle vibrational calculations, at least with 6-31G* or comparable basis sets, were hardly feasible for larger systems such as exohedral fullerene derivatives, since in these cases the increased number of atoms was typically accompanied by a symmetry reduction. The increased computational demands were prohibitive for these molecules since the interpretation of the spectra of lower symmetrical compounds requires a more accurate prediction of vibrational frequencies and relative intensities than for the parent fullerenes. The use of smaller basis sets (such as 3-21G) with Hartree–Fock or density functional theory (DFT) methods,^{25,26} as well as application of semiempirical methods either of MNDO-²² or tight-binding types,^{24,27,31,32} resulted in computational data of sufficient accuracy to provide a qualitative understanding of the vibrational structure but did not allow peak-to-peak assignment of the whole set of experimental data. Taking advantage of the density fitting technique,³⁷ which allows considerable acceleration of pure DFT computations, we have applied the PBE³⁸/TZ2P approach to interpret vibrational spectra of polymeric C_{60} ,^{29,30} and bromo-³⁹ and chlorofullerenes.^{35,36} The method was found to be quite accurate in predictions of the carbon cage vibrations, while the frequencies of C–Hal bending and stretching modes were underestimated. However, due to the systematic character of these errors they could be effectively corrected with the use of the scaling procedure of Pulay et al.⁴⁰ Recently, we have succeeded in the measurement and DFT-based interpretation of the $\text{C}_{60}\text{F}_{20}$ IR and Raman spectra, which in turn provided unambiguous structural assignment for the D_{5d} - $\text{C}_{60}\text{F}_{20}$ isomer isolated from the metal–fluoride reaction product.³⁴ Some IR and Raman spectroscopic data on $\text{C}_{60}\text{F}_{36}$ and $\text{C}_{60}\text{F}_{48}$ have been previously reported,^{16,41}

but none of those studies included reliable interpretation of the spectroscopic data or the use of vibrational spectra for structure elucidation. The only attempt of this sort was reported by Fowler et al. who computed IR spectra of the D_3 and S_6 isomers, but the accuracy of the semiempirical MNDO method used in that work was not sufficient for distinguishing these isomers.¹²

In this work, we apply vibrational spectroscopic methods in combination with the theoretical analysis for the elucidation of the molecular structures of $\text{C}_{60}\text{F}_{48}$ and C_3 - $\text{C}_{60}\text{F}_{36}$. We report that comprehensive IR and Raman spectroscopic studies of $\text{C}_{60}\text{F}_{48}$ combined with the DFT vibrational simulations can distinguish D_3 and S_6 isomers of $\text{C}_{60}\text{F}_{48}$ and thus confirm earlier structural assignment of the major isomer to D_3 symmetric structure and identify characteristic spectral features of the minor S_6 structure. This work provides detailed vibrational assignments for D_3 - $\text{C}_{60}\text{F}_{48}$ and C_3 - $\text{C}_{60}\text{F}_{36}$ fluorofullerenes.

Experimental Section

The samples of $\text{C}_{60}\text{F}_{48}$ were synthesized by direct C_{60} fluorination using the following procedure. Finely ground C_{60} powder was placed in the Ni boat and was treated with the F_2/Ar (1:7) gas flow for 24 h at $350\text{ }^\circ\text{C}$ (see also ref 42). Electrospray ionization mass spectrometric analysis (ESI MS) showed the compositional purity to be 95+%; ^{19}F NMR data indicated (from integrated peak intensities) that 85% of the solid sample consisted of the major isomer, the minor isomer (also with eight equal-intensity lines in F NMR) constituted 5–7%, and the remaining ca. 8% could be accounted for the $\text{C}_{60}\text{F}_{46}$ admixture, which is also indicated by mass spectrometry. Several batches of the $\text{C}_{60}\text{F}_{36}$ samples were used in this study. They were prepared by the MnF_3 method at 350 – $400\text{ }^\circ\text{C}$.¹⁶ HPLC analysis detected very little presence (if any) of C_{60} or $\text{C}_{60}\text{F}_{18}$, and those samples were used without further purification. Some samples (prepared at higher temperatures) were subjected to subsequent sublimation ($290\text{ }^\circ\text{C}$) in order to separate less volatile impurities of unreacted C_{60} and/or $\text{C}_{60}\text{F}_{18}$.

FT-Raman spectra were measured on a Bruker RFS 100 spectrometer (excitation with 1064 nm line of Nd:YAG laser; power, 120 mW; resolution, 3 cm^{-1} for $\text{C}_{60}\text{F}_{48}$ and 1 cm^{-1} for $\text{C}_{60}\text{F}_{36}$; 1000 scans were accumulated). Raman spectra excited by the 676.4 nm line of the Kr^+ laser were measured on a Dilor XY triple grating spectrometer with CCD detection; spectra were recorded in a subtractive mode using micro-Raman sampling at 1.5 cm^{-1} resolution averaging 30 accumulations of 15 s integration. IR spectra were measured on a Bruker Equinox 55 FT-IR spectrometer. Samples for IR measurements were either pressed pellets of pure fluorofullerenes (1–1.5 mg of the compound pressed into a 3 mm diameter pellet) or pressed pellets of fluorofullerenes diluted with KBr (typically, 0.5 mg of fluorofullerene dispersed in 20 mg of KBr). Resolution was set to 1 cm^{-1} for mid-IR range and 2 cm^{-1} for far-IR range; 128 scans were accumulated.

Computational Details

Force fields and IR intensities were calculated at the DFT level of theory with the PRIRODA package³⁷ using Perdew–Burke–Ernzerhof (PBE) functional³⁸ and implemented TZ2P-quality basis set. The quantum-chemical code employed expansion of the electron density in an auxiliary basis set to accelerate evaluation of the Coulomb and exchange–correlation terms. DFT force fields were transferred into redundant internal coordinate systems comprising all chemical bonds and angles and scaled with the use of scaling factors transferred from the $\text{C}_{60}\text{F}_{20}$ molecule.³⁴ Raman intensities were computed numeri-

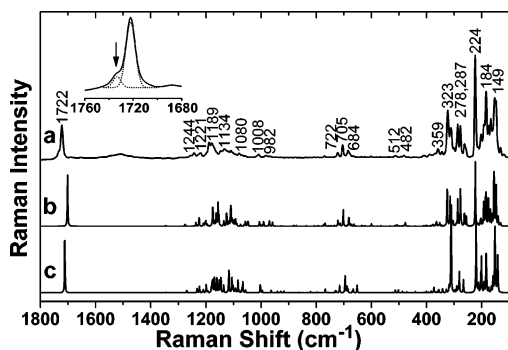


Figure 2. (a) Raman spectrum of C₆₀F₄₈ (1064 nm); calculated Raman spectra for (b) *D*₃ and (c) *S*₆ isomers. Inset shows the $\nu(\text{C}=\text{C})$ range; the arrow denotes the spectral feature assigned to the *S*₆ isomer. The broad band at 1500 cm⁻¹ in the experimental spectrum belongs to unidentified impurity.

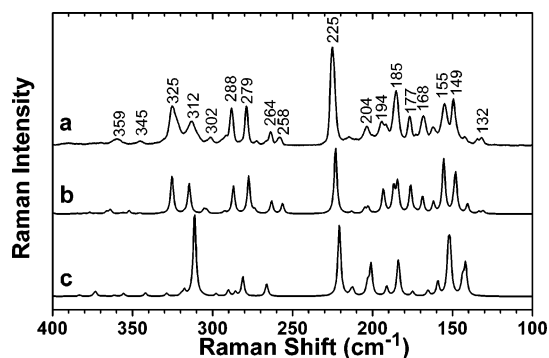


Figure 3. (a) Experimental Raman spectrum of C₆₀F₄₈ (676.4 nm); calculated Raman spectra for (b) *D*₃ and (c) *S*₆ isomers.

cally at the HF/6-31G level using the PC version⁴³ of the GAMESS (U.S.) package.⁴⁴ Force field scaling and potential energy distribution (PED) analysis were performed using the DISP suite of programs.⁴⁵

Results and Discussion

Identification of *D*₃ and *S*₆ Isomers of C₆₀F₄₈. According to group theory, vibrations of C₆₀F₄₈ isomers span the following irreducible representations:

$$\Gamma_{\text{vib}}(D_3\text{-C}_{60}\text{F}_{48}) = 54A_1(\text{R}) + 52A_2(\text{IR}) + 106E(\text{IR},\text{R})$$

$$\Gamma_{\text{vib}}(S_6\text{-C}_{60}\text{F}_{48}) = 53A_g(\text{R}) + 53E_g(\text{R}) + 53A_u(\text{IR}) + 53E_u(\text{IR})$$

where (R) and (IR) designate Raman and IR activity, respectively. Accordingly, more than 100 modes are expected in the IR and Raman spectra of both isomers. It is noteworthy that the E modes of the *D*₃ isomer are both IR- and Raman-active, whereas spectra of the *S*₆ isomer should obey the rule of mutual exclusion.

The Raman spectrum of C₆₀F₄₈ is compared to the simulated spectra for *D*₃ and *S*₆ isomers in Figure 2. Although at first sight both calculated spectra appear to reproduce the topology of the experimental spectrum equally well, a more detailed analysis of the 100–400 cm⁻¹ region, where the strongest Raman lines are observed, allows a clear distinction between the calculated *D*₃ and *S*₆ spectra to be made (Figure 3). In the 250–350 cm⁻¹ region of the experimental spectrum, four medium bands at 279, 288, 312, and 325 cm⁻¹ and weaker features at 258, 264, 273, and 302 cm⁻¹ are observed. A simulated spectrum of the *D*₃ isomer reproduces each of these

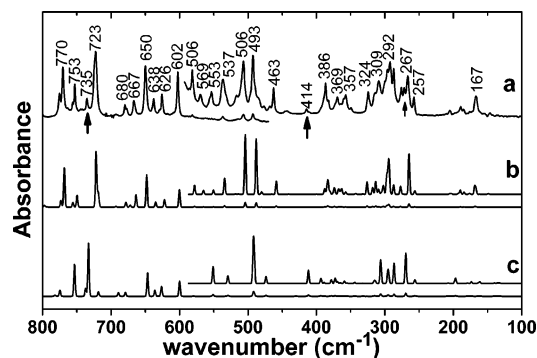


Figure 4. (a) Experimental IR spectrum of C₆₀F₄₈ in the 100–800 cm⁻¹ range; calculated IR spectra for (b) *D*₃ and (c) *S*₆ isomers. Arrows denote spectral features assigned to the *S*₆ isomer.

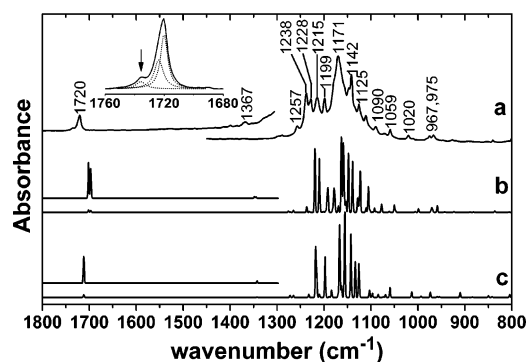


Figure 5. (a) Experimental IR spectrum of C₆₀F₄₈ in the 800–1800 cm⁻¹ range; calculated IR spectra for (b) *D*₃ and (c) *S*₆ isomers. Inset shows the $\nu(\text{C}=\text{C})$ range; the arrow denotes the spectral feature assigned to the *S*₆ isomer.

experimental peaks to within 3–4 cm⁻¹, whereas the simulated spectrum of the *S*₆ isomer fails to provide a match in this range.

The calculated IR spectra of the C₆₀F₄₈ isomers also provide sufficient information allowing us to distinguish *D*₃ and *S*₆ isomers. Figure 4 shows the experimental and calculated IR spectra of C₆₀F₄₈ in the 100–800 cm⁻¹ range. Even prior to comparison with the computed spectra, the centrosymmetric *S*₆ structure can be discarded on the basis of the mutual exclusion rule since several experimental Raman bands have their counterparts in the far-IR spectrum, albeit with much lower relative intensities. Comparison of the calculated and experimental IR spectra (Figures 4 and 5) also unambiguously favors the *D*₃ structure. According to potential energy distribution analysis (see Supporting Information), normal modes of C₆₀F₄₈ below 800 cm⁻¹ have complex forms involving a mixture of C–F bends and radial cage displacements (mostly in CC(F)C angles). Clear distinction between the spectra of very similar isomers is another manifestation of the ultimate structural sensitivity of the carbon cage radial modes that was already demonstrated in our previous work on C₆₀F₂₀.³⁴

The range of $\nu(\text{C}-\text{F})$ stretching modes can hardly be expected to be structure sensitive due to the very high density of vibrational modes arising from 48 C–F bonds. The situation is additionally complicated by their mixing with the stretching C(F)–C(F) vibrations which also occur in the same frequency range. However, the strong $\nu(\text{C}-\text{F})$ absorption of C₆₀F₄₈ has well-defined fine structure (Figure 5; see also refs 9 and 41), which is reasonably well reproduced by the computed spectrum of the *D*₃ isomer. This is best illustrated in the range from 1150 to 1300 cm⁻¹, where the experimental spectrum exhibits a system of four strong lines at 1199, 1215, 1228, and 1238 cm⁻¹ with a weaker band at 1257 cm⁻¹. This pattern is perfectly

reproduced in the simulated spectrum of the D_3 isomer, while only two intense bands are predicted for the S_6 isomer. C–F bonds in $C_{60}F_{48}$ can be divided into two groups according to their neighborhood: (1) those with two and (2) those with three C(sp³) neighbors. Our calculations (and experimental X-ray data¹⁰) have shown that different topology results in substantial alteration in the bond lengths, being 1.387–1.392 Å for the first and 1.368–1.374 Å for the second group. In the vibrational spectra these alterations manifest themselves in an almost perfect separation of the longer and shorter bonds' modes, the former appearing at 1070–1170 cm⁻¹ with the latter at 1170–1240 cm⁻¹.

Comparison of the experimental and computed IR and Raman spectra of $C_{60}F_{48}$ unambiguously demonstrates that the D_3 isomer is the major component of the product. According to NMR data, it constitutes 85%, whereas the S_6 structure is present in the amount of ca. 10%, which is in principle detectable by vibrational spectroscopy. We found several IR features that can be assigned to the S_6 isomer (see Supporting Information for a complete list). Due to overlap with the strong absorptions of the major isomer, S_6 bands mostly appear as shoulders and their assignment is somewhat difficult, except for those at 272, 414, and 735 cm⁻¹ (see arrows in Figure 4) which appear as resolved peaks. Whereas the 272 and 414 cm⁻¹ features are rather weak and also require special experimental equipment for the far-IR measurements, the 735 cm⁻¹ line is accessible by all IR spectrometers and hence may be used for analytical purposes. In the Raman spectra the only clearly resolved feature of the S_6 isomer is found in the $\nu(C=C)$ range. According to our calculations, C=C bonds of the S_6 isomer are 0.0026 Å shorter than in the D_3 , and $\nu(C=C)$ frequencies of the S_6 should be 10–12 cm⁻¹ higher than those of the D_3 isomer. In the experimental spectra, C=C stretching modes of D_3 are observed at 1720/1724 (IR, weak) and 1722 cm⁻¹ (Raman, medium), whereas shoulders at 1733 (Raman, Figure 2 inset) and 1736 cm⁻¹ (IR, see arrow in Figure 5 inset) can be reliably assigned to the S_6 structure.

Stability of $C_{60}F_{36}$ Isomers. Uncertainties with NMR data on the C_3 isomer of $C_{60}F_{36}$ ^{46,47} has provoked several theoretical studies of $C_{60}F_{36}$ isomers with the aim to find the most stable ones. The broadest selection of isomers was considered by Clare and Kepert,^{48,49} who have studied more than 100 isomers of $C_{60}F_{36}$ in their works. The most recent NMR analysis on C_3 - $C_{60}F_{36}$ shows the best match to the most stable C_3 isomer of all those calculated to date, which has three isolated benzenoid rings (IBRs) and three isolated double bonds in its structure.⁷ C_1 - $C_{60}F_{36}$, as found by X-ray single-crystal analysis, has nearly the same structure with only one double bond “migrated” to the adjacent position.¹⁷ This C_1 isomer was also found to be among the most stable structures of $C_{60}F_{36}$ ¹⁷ and $C_{60}H_{36}$.⁵⁰ Thus, all three isomers of $C_{60}F_{36}$ isolated so far (T , C_3 , C_1) seem to be the most stable structures of this composition—at least among the hundreds of studied isomers. This is in line with other examples of multiply functionalized fullerenes ($C_{60}H_{36}$,^{50,51} $C_{60}H_{18}$,⁵² $C_{60}F_{18}$,⁵³ $C_{60}Cl_{28}$,⁵⁴ $C_{70}F_{38}$,⁵⁵ $C_{60}Cl_{30}$,⁵⁶ $C_{70}Cl_{28}$,⁵⁷ $C_{74}F_{38}$,⁵⁸ $C_{78}Br_{18}$,⁵⁹ and $C_{84}F_{40}$ ⁶⁰), which all demonstrate that formation of the IBRs is a very important stabilizing factor for these derivatives. However, without an exhaustive search of all possible isomers for a given composition, no guarantee can be provided that all the most stable isomers were identified.

In search of the other possible stable structures for $C_{60}F_{36}$, we have considered a much broader selection of isomers, which involved all structures with three IBRs (the case with four IBRs is trivial since there is only one way to locate four IBRs on C_{60}

and it is realized in T - $C_{60}F_{36}$). Three IBRs can be located on the C_{60} surface in two different ways. One motif (series I, Figure S1a of the Supporting Information) is just a substructure of the T isomer, while another one (series II, Figure S1b of the Supporting Information) comprises C_s symmetric arrangement of IBRs (to our knowledge, this motif has not been considered previously). Each motif with three IBRs allows hundreds of variants for location of the three remaining C=C bonds, and it is not possible to perform calculations for all these structures at the DFT level at the present time.

It was shown earlier⁴⁹ that semiempirical AM1 method substantially underestimates the stability enhancement provided by IBRs, and therefore relative energies for isomers with different numbers of IBRs are not very reliable. However, for the isomers with the same number of IBRs relative AM1 energies are close to the DFT ones, which allows one to use the semiempirical method for exploratory search of the stable isomers. Using the AM1 method, we have performed computations for all possible isomers of $C_{60}F_{36}$ (total of 261 structures in series I and 390 in series II; see Supporting Information for complete list of the isomers and their relative energies). Then, DFT//AM1 single-point energies were computed for all stable isomers in the 100 kJ/mol range (26 isomers), and finally, full geometry optimization was performed at the DFT level for the 9 most favored isomers (Table S5 of the Supporting Information).

In agreement with the earlier results, T - $C_{60}F_{36}$ with four IBRs is the most stable isomer at the DFT level,^{49,61} followed by C_3 - $C_{60}F_{36}$ (isomer N64) (PBE/TZ2P relative energy 10.7 kJ/mol) and X-ray characterized C_1 - $C_{60}F_{36}$ (16.9 kJ/mol). Similar values were obtained for these three isomers at the B3LYP/6-31G* level,¹⁷ the relative energies of C_3 (N64) and C_1 isomers being 11.5 and 18.4 kJ/mol, respectively. In the whole set of the calculated isomers, these three structures demonstrate outstanding stability and are separated from all others by the gap of 30 kJ/mol (i.e. relative energy of the fourth most stable isomer is 47.4 kJ/mol). The relative energy of the C_3 (N3) isomer, which was considered in ref 46 on mechanistic grounds, is 270.4 kJ/mol. Note that the isomers with two IBRs were not studied in this work. The total number of such isomers may exceed 2×10^5 , and it is hardly possible to compute formation enthalpies for all of them even at the AM1 level. The most stable isomer of $C_{60}F_{36}$ with two IBRs found so far by the others— S_6 (N88)—is 46.5 kJ/mol less stable than T - $C_{60}F_{36}$ at the B3LYP/6-31G**/AM1 level.⁴⁹

Isomeric Composition of the $C_{60}F_{36}$ Samples. In this work, the experimental vibrational study was done not on the pure $C_{60}F_{36}$ isomers but on the as-prepared samples. We did not use HPLC isolation of pure isomers of $C_{60}F_{36}$ for the following reasons: (1) this procedure notoriously results in the significant sample degradation on the column producing numerous oxides and hydroxides;⁶² (2) as demonstrated,⁷ the presence of the T isomer was much lower than that of the C_3 isomer ($T:C_3 = 1:10$ – 15) in all samples, so it was not expected to significantly interfere with our spectroscopic studies, under the assumption that the C_3 isomer constitutes 90–93 mol % in the samples. However, our analysis of ¹⁹F NMR spectra performed for a dozen of the crude $C_{60}F_{36}$ samples of different origin showed that they contained not only the expected 12 + 3 lines due to C_3 and T isomers but the third component with ca. 36 equal-intensity lines was present comprising as much as 25–30% of the total F signals. For example, one of the typical samples contained 65 mol % of the C_3 isomer of $C_{60}F_{36}$, less than 3 mol % of the T isomer, while the remainder of the integrated F signal

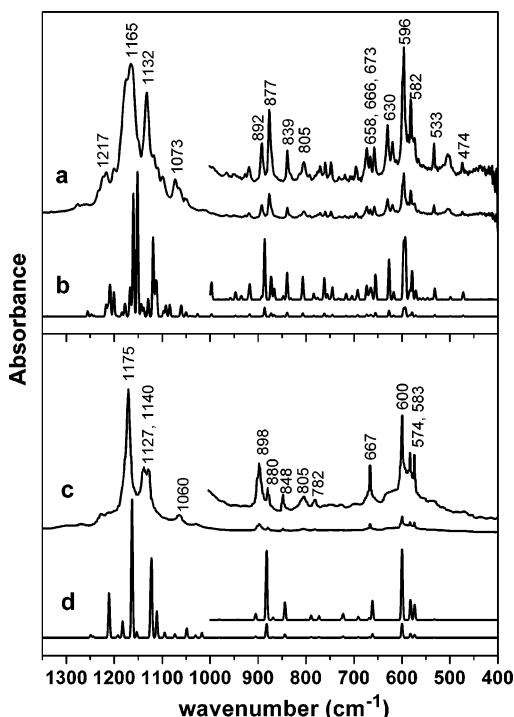


Figure 6. IR spectra of C₃-C₆₀F₃₆: (a) 90+ mol % sample from this work; (b) calculated IR spectrum of C₃(N64)-C₆₀F₃₆. IR spectra of T-C₆₀F₃₆: (c) experimental spectrum from ref 46; (d) calculated IR spectrum for T-C₆₀F₃₆. Wavenumbers in the experimental spectrum of the T isomer are arbitrary within 5 cm⁻¹.

intensity constituted almost 28 mol % of the third component. Using a recrystallization technique, we were able to partially purify one crude sample to ca. 90 mol % of C₃-C₆₀F₃₆, and for such a compound a mid-IR spectrum was recorded (see Figure 6a). However, data on the overall composition of the crude samples and identification of the third component were needed for interpretation of the Raman and far-infrared data.

Apparently, this third component has low symmetry and could be assigned to either an oxide (C₆₀F₃₆O or C₆₀F₃₄O), hydroxide, or nonsymmetric C₆₀F₃₈. However, a close inspection of the mass spectral data did not show the presence of oxides or species with higher F content in any appreciable amounts that could account for almost 30% in the samples. In addition, comparison of the ¹⁹F NMR spectra of our samples with those of the purified C₆₀F₃₄O,⁶² C₁-C₆₀F₃₈,⁶³ C₆₀F₃₅OH,⁶⁴ and C₁-C₆₀F₃₆¹⁷ allows us to conclude that, in fact, the third component and the second most abundant component in the crude C₆₀F₃₆ samples is the C₁ isomer of C₆₀F₃₆. We were not able to perform direct comparison of our NMR spectra with that of the reported C₁ isomer because the precise conditions of the NMR experiment in ref 17 are not given. Further complication brings the fact that the nature/composition of the NMR solvent affects the absolute values of the chemical shifts in these compounds; especially significant changes in different solvents were observed in the -140 to -150 ppm region.⁷ Nevertheless, the relative positions of most of the corresponding NMR peaks were found to be very close; especially convincing is the comparison of the presented reference 6:1 mixture of C₃:C₁ isomers obtained after partial conversion of pure C₁-C₆₀F₃₆ (see Figure 7) to the crude samples obtained in this work and earlier¹⁶ (see more in the Supporting Information).

Thus, the study of the isomeric compositions of several crude samples of C₆₀F₃₆ demonstrate that the relative abundance of the three C₆₀F₃₆ isomers is highly reproducible regardless of the differences in reaction conditions, and it follows that C₃ >

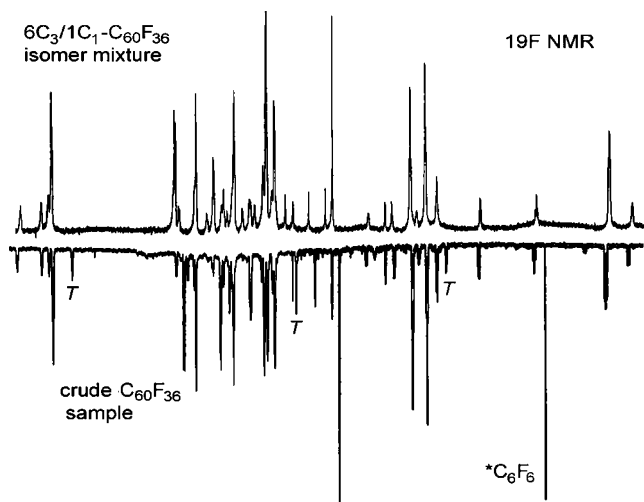


Figure 7. Comparison of the ¹⁹F NMR spectra of the 6:1 C₃:C₁-C₆₀F₃₆ mixture from ref 64 and the crude C₆₀F₃₆ sample used in this work.

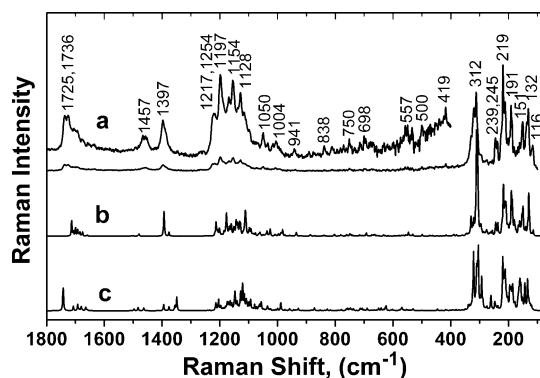


Figure 8. (a) Experimental Raman spectrum of C₆₀F₃₆ (1064 nm); (b) calculated Raman spectrum of the 2:1 C₃(N64)/C₁ mixture; (c) calculated Raman spectrum of the 2:1 C₃(N3)/C₁ mixture.

C₁ >> T. Similarly to the case of hydrogenated fullerene, C₆₀H₃₆,⁵¹ this order does not exactly follow DFT-calculated relative thermodynamic stabilities (formation enthalpies) of the respective isomers T(0 kJ/mol) > C₃(10.6 kJ/mol) > C₁ (16.9 kJ/mol), which can be tentatively explained by the entropy difference effect, which favors less symmetric species formation. On the other hand, we also found that some enhancement in the relative content of the most stable T isomer occurs when either the higher temperature of synthesis or that of resublimation was applied. This may indicate that equilibrium isomeric composition has not yet been reached at lower temperatures.

Vibrational Assignment for C₆₀F₃₆. Vibrations of C₃-C₆₀F₃₆ span 94A(IR,R) + 94E(IR,R) irreducible representations, resulting totally in 188 either IR and Raman active modes. Groups theory analysis for C₁-C₆₀F₃₆ is trivial with all its 282 modes being both IR and Raman active. As can be anticipated from these numbers, experimental vibrational spectra of the C₆₀F₃₆ sample are rather complex with more than 100 detectable bands. Nevertheless, computed spectra of the 2:1 C₃(N64)/C₁ mixture almost perfectly reproduce experimental frequencies with average errors less than 5 cm⁻¹ (except for the ν(C-F) range, where computed frequencies are systematically lower at ca. 20 cm⁻¹), while simulated spectra of the 2:1 C₃(N3)/C₁ mixture cannot account for all features observed in the experimental spectra (Figures 8–10). Thus, our data confirm previous structural assignment for C₃-C₆₀F₃₆, and reliable assignment of the experimental vibrational spectra can be performed now. While vibrational frequencies of C₆₀F₃₆ are continuously distributed

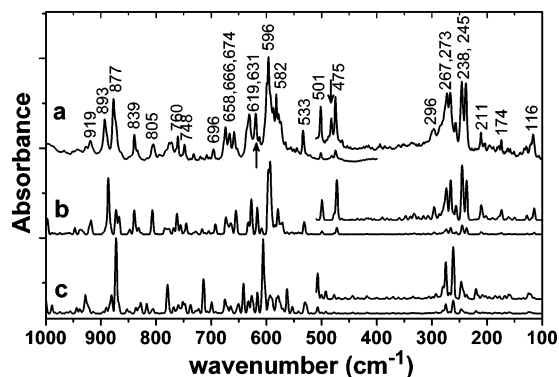


Figure 9. (a) Experimental IR spectrum of $C_{60}F_{36}$ in the 100–1000 cm^{-1} range; (b) calculated IR spectrum of the 2:1 $C_3(N64)/C_1$ mixture; (c) calculated IR spectrum of the 2:1 $C_3(N3)/C_1$ mixture. The arrows in the experimental spectrum denote the features assigned to the C_1 isomer.

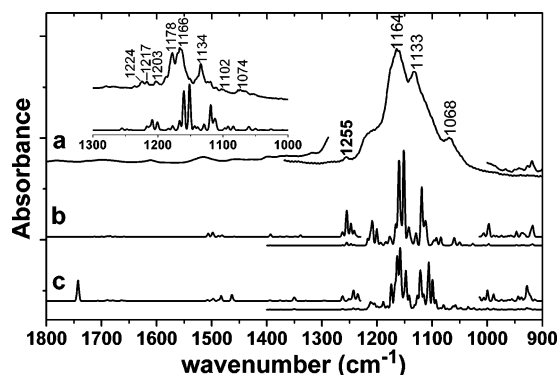


Figure 10. (a) Experimental IR spectrum of $C_{60}F_{36}$ in the 900–1800 cm^{-1} range; (b) calculated IR spectrum of the 2:1 $C_3(N64)/C_1$ mixture; (c) calculated IR spectrum of the 2:1 $C_3(N3)/C_1$ mixture. The inset shows the IR spectrum of the matrix isolated $C_{60}F_{36}$ from ref 41 in comparison to the calculated spectrum of the $C_3(N64)$ isomer.

in the 100–1750 cm^{-1} range, distribution of the IR and Raman intensities is not uniform with several domains formed, which we will analyze further in this section.⁶⁵

The range of 100–400 cm^{-1} is characterized by strong Raman and very modest IR intensity. According to the PED analysis, most of the modes below 400 cm^{-1} have a prevailing (50–80%) contribution of the C–F bends, partially mixed with the carbon cage radial deformations. The latter resemble the squashing H_g mode of the parent fullerene, most likely owing a part of their Raman intensity to this fact. At the higher frequencies (400–900 cm^{-1}), CCF contributions decrease to 30–40%, while contribution of CC(F)C bends rise to 20–30%. Starting from 700 cm^{-1} , stretching C(F)–C(F) modes also contribute ca. 10–15% to some modes. Raman scattering is nearly silent in the 400–900 cm^{-1} range, with only a few weak features hardly distinguishable from the background noise, but the IR spectrum of $C_{60}F_{36}$ comprises a wealth of medium well-resolved peaks, which are perfectly reproduced by the computed spectrum.

In the range of $\nu(C-F)$ stretching modes, room-temperature IR spectrum shows one broad band with a maximum at 1164 cm^{-1} and shoulder features at 1068, 1133, and around 1210 cm^{-1} . Much better resolution for these modes was obtained in the C_3 -enriched sample (Figure 6a) or in ref 41 for the matrix-isolated $C_{60}F_{36}$ at 12 K (Figure 10, inset), and we will use those data in the further analysis (see Table S9 of the Supporting Information). The room-temperature Raman spectrum also shows rather fine structure in this range. Computed frequencies

underestimate the experimental ones at ca. 20 cm^{-1} , but the whole pattern is still satisfactorily reproduced, so that well-resolved low-temperature data can be analyzed with some confidence. As in the case of $C_{60}F_{48}$, C–F bonds in $C_{60}F_{36}$ can be classified into different groups according to their topology and lengths: (1) 9 bonds with three C(sp^3) neighbors and lengths of 1.362, 1.364, and 1.366 Å; (2) 24 bonds with two C(sp^3) neighbors, falling into the 1.379–1.395 Å range; (3) three bonds with only one C(sp^3) neighbor and the length of 1.396 Å. As follows from the PED analysis, IR and Raman bands at 1217 and 1224 cm^{-1} are due to the stretching modes of C–F bonds with three C(sp^3) neighbors, while the peaks at 1100–1200 cm^{-1} are due to the longer C–F bonds.

Stretching vibrations of the ordinary carbon–carbon bonds have very low IR and Raman activity and appear in the spectra only as admixtures to C–F stretches (this maxim mostly concerns the longest C(F)–C(F) bonds). C(sp^2)–C stretches fall into the 1240–1400 cm^{-1} interval, partially mixed with CC(F)C (below 1250 cm^{-1}) or C=C–C deformations (1300–1400 cm^{-1}) and are not detected in the experimental spectra. CC stretches in benzene rings are predicted to be at 1390–1680 cm^{-1} , and in the experimental spectra they appear as a weak broad IR band at 1516 cm^{-1} , medium Raman line at 1397 cm^{-1} and a few weak Raman features at 1457, 1695, and 1707 cm^{-1} . C=C stretches do not appear in the IR spectrum as well, while in the Raman spectrum they constitute a doublet at 1725/1736 cm^{-1} .

T Isomer of $C_{60}F_{36}$. ^{19}F NMR data have shown only a marginal presence of the T - $C_{60}F_{36}$ in our sample, and its characteristic vibrations are hidden in the more complex spectral pattern of the less symmetric isomers. However, earlier, one of us⁴⁶ succeeded in the isolation of the T and C_3 isomers by three-stage HPLC procedure, and IR spectra of isomerically pure samples could be measured. The IR spectrum of the C_3 isomer from ref 46 corresponds well to our Figure 6a, while the mid-IR spectrum of the T isomer from ref 46 is compared to the results of our calculations in Figure 6c,d. As in the case of the C_3 isomer, the scaled DFT spectrum provides a very good match to the experimental data. The IR spectrum of the T - $C_{60}F_{36}$ is much simpler compared to that of the C_3 - $C_{60}F_{36}$, which naturally follows from the higher symmetry (vibrations of the T isomer span 24 A(R) + 24E(R) + 70F(IR,R) irreducible representations). At the same time, the overall spectral patterns for these molecules are very similar, and normal-mode analysis given above for C_3 - $C_{60}F_{36}$ is valid for T - $C_{60}F_{36}$ as well, excluding the C=C stretching range since isolated double bonds are absent in the latter.

Conclusions

Experimental vibrational spectroscopy in conjunction with DFT quantum chemical calculations was applied to characterize two fluorofullerenes, $C_{60}F_{48}$ and $C_{60}F_{36}$. Excellent agreement between the experimental and DFT-computed IR and Raman spectra allowed us to distinguish the very similar D_3 and S_6 isomers of $C_{60}F_{48}$. Our study shows that vibrational spectroscopy, supplemented with reliable theoretical modeling, can provide a powerful structural tool to meet the challenges of the structure determination for fullerene derivatives when other methods, such as X-ray or NMR are unable to provide unambiguous solutions to the problem. Richness, intensity, and high structural sensitivity of the Raman spectra in the 100–400 cm^{-1} range and IR spectra in the 400–900 cm^{-1} range endorse these spectral ranges as fingerprints of the different fluorofullerene molecules. Mixing of the carbon cage vibrations

with C–F bending modes results in a change in the spectral pattern of fluorofullerenes compared to that of fullerenes, which is the most evident as a considerable downshift of the strong Raman modes. Besides, isolated double bonds in the fluorofullerenes are very short and thus have unusually high stretching frequencies, ca. 100 cm⁻¹ above the normal values. Finally, detailed interpretation of the vibrational spectra of D₃-C₆₀F₄₈ and C₃-C₆₀F₃₆ isomers proposed in this work represents a rare example of the vibrational assignment for molecules of this size.

Acknowledgment. This work was supported by the Volkswagen Foundation (Grant I-77/855) and Humboldt Foundation (F. Bessel award to O.V.B.). Computer time at the Research Computing Center of the Moscow State University is gratefully acknowledged. The authors are thankful to Igor Kuvychnko for some NMR measurements and Dr. I. V. Goldt for assistance in preparing some of the C₆₀F₃₆ samples. O.V.B. thanks S. H. Strauss for insightful discussions. R.N.C. is indebted to the NSF for partial support.

Supporting Information Available: DFT-optimized Cartesian coordinates of C₆₀F₄₈ and C₆₀F₃₆ isomers, computed AM1 and DFT energies of all C₆₀F₃₆ isomers with three isolated benzenoid rings, a complete list of S₆-C₆₀F₄₈, T-C₆₀F₃₆, and C₁-C₆₀F₃₆ calculated frequencies and intensities; comparison of the computed IR and Raman spectra of T, C₃, and C₁ isomer of C₆₀F₃₆, PED normal-mode analysis for D₃-C₆₀F₄₈ and C₃-C₆₀F₃₆, and ¹⁹F NMR spectra of the crude and purified samples of C₆₀F₃₆.

References and Notes

- Boltalina, O. V.; Strauss, S. H. Fluorofullerenes. In *Encyclopedia on Nanoscience and Nanotechnology*; Schwarz, J. A., Contescu, C., Putyera, K., Eds.; Dekker: New York, 2003; pp 1175–1190.
- Hackermüller, L.; Uttenthaler, S.; Hornberger, K.; Reiger, E.; Brezger, B.; Zeilinger, A.; Arndt, M. *Phys. Rev. Lett.* **2003**, *91*, 090408.
- Strobel, P.; Riedel, M.; Ristein, J.; Ley, L.; Boltalina, O. *Diamond Relat. Mater.* **2005**, *14*, 451–458.
- Goldt, I. V.; Boltalina, O. V.; Kemnitz, E.; Troyanov, S. I. *Solid State Sci.* **2002**, *4*, 1395–1401.
- Lukonin, A. Y.; Markov, V. Y.; Boltalina, O. V. *Vestn. Mosk. Univ., Ser. 2: Khim.* **2001**, *42*, 3–16.
- Bagryantsev, V. F.; Zapol'skii, A. S.; Boltalina, O. V.; Galeva, N. A.; Sidorov, L. N. *Zh. Neorg. Khim.* **2000**, *45*, 1121–1127.
- Gakh, A. A.; Tuinman, A. A. *Tetrahedron Lett.* **2001**, *42*, 7137–7139.
- Gakh, A. A.; Tuinman, A. A.; Adcock, J. L.; Sachleben, R. A.; Compton, R. N. *J. Am. Chem. Soc.* **1994**, *116*, 819–820.
- Boltalina, O. V.; Galeva, N. A. *Russ. Chem. Rev.* **2000**, *69*, 609–621.
- Troyanov, S. I.; Troshin, P. A.; Boltalina, O. V.; Ioffe, I. N.; Sidorov, L. N.; Kemnitz, E. *Angew. Chem., Int. Ed.* **2001**, *40*, 2285–2287.
- Neretin, I. S.; Lyssenko, K. A.; Antipin, M. Yu.; Slovokhotov, Yu. L. *Russ. Chem. Bull.* **2002**, *51*, 695–703.
- Austin, S. J.; Fowler, P. W.; Sandall, J. P. B.; Zerbetto, F. *J. Chem. Soc., Perkin Trans. 2* **1996**, 155–158.
- Cioslowski, J.; Rao, N.; Szarecka, A.; Pernal, K. *Mol. Phys.* **2001**, *99*, 1229.
- Hedberg, L.; Hedberg, K.; Boltalina, O. V.; Galeva, N. A.; Zapol'skii, A. S.; Bagryantsev, V. F. *J. Phys. Chem. A* **2004**, *108*, 4731–4736.
- Boltalina, O. V.; Markov, V. Y.; Lukonin, A. Y.; Avakjan, T. V.; Ponomarev, D. B.; Sorokin, I. D.; Sidorov, L. N. In *Recent Advances in the Chemistry and Physics of Fullerenes and Related Materials*; Kadish, K. M., Ruoff, R. S., Eds.; Electrochemical Society: Pennington, NJ, 1995; pp 1395–1408.
- Boltalina, O. V.; Borschevskii, A. Y.; Sidorov, L. N.; Street, J. M.; Taylor, R. *Chem. Commun. (Cambridge)* **1996**, 529–530.
- (a) Avent, A. G.; Clare, B. W.; Hitchcock, P. B.; Kepert, D. L.; Taylor, R. *Chem. Commun. (Cambridge)* **2002**, 2370–2371. (b) Hitchcock, P. B.; Taylor, R. *Chem. Commun. (Cambridge)* **2002**, 2078–2079.
- Schettino, V.; Pagliai, M.; Ciabini, L.; Cardini, G. *J. Phys. Chem. A* **2001**, *105*, 11192–11196.
- Menendez, J.; Page, J. B. *Light Scattering in Solids VIII*. Topics in Applied Physics; Springer-Verlag: Berlin, Heidelberg, Germany, 2000; Vol. 76, pp 27–95.
- Schettino, V.; Pagliai, M.; Cardini, G. *J. Phys. Chem. A* **2002**, *106*, 1815–1823, and references therein.
- Bettinger, H. F.; Scuseria, G. E. *Chem. Phys. Lett.* **2000**, *332*, 35–42.
- Kuzmany, H.; Plank, W.; Winter, J.; Dubay, O.; Tagmatarchis, N.; Prassides, K. *Phys. Rev. B* **1999**, *60*, 1005–1012.
- Krause, M.; Hulman, M.; Kuzmany, H.; Dennis, T. J. S.; Inakuma, M.; Shinohara, H. *J. Chem. Phys.* **1999**, *111*, 7976–7984.
- Krause, M.; Kuzmany, H.; Georgi, P.; Dunsch, L.; Vietze, K.; Seifert, G. *J. Chem. Phys.* **2001**, *115*, 6596–6605.
- Kobayashi, K.; Nagase, S. *Mol. Phys.* **2003**, *101*, 249–254.
- Shimotani, H.; Ito, T.; Iwasa, Y. T., A.; Shinohara, H.; Nishibori, E.; Takata, M.; Sakata, M. *J. Am. Chem. Soc.* **2004**, *126*, 364–369.
- Long, V. C.; Musfeldt, J. L.; Kamaras, K.; Adams, G. B.; Page, J. B.; Iwasa, Y.; Mayo, W. E. *Phys. Rev. B* **2000**, *61*, 13191–13201.
- Davydov, V. A.; Kashevarova, L. S.; Rakhmanina, A. V.; Senyavin, V. M.; Ceolin, R.; Szwarc, H.; Allouchi, H.; Agafonov, V. *Phys. Rev. B* **2000**, *61*, 11936–11945.
- Senyavin, V. M.; Popov, A. A.; Granovsky, A. A.; Davydov, V. A.; Agafonov, V. N. *Fullerenes, Nanotubes, Carbon Nanostruct.* **2004**, *12*, 253–258.
- Senyavin, V. M.; Popov, A. A.; Granovsky, A. A. Vibrational spectra of C₆₀ polymers: Experiment and first-principle assignment. In *Hydrogen Materials Science and Chemistry of Carbon Nanomaterials*; Veziroglu, T. N., et al., Eds.; NATO Science Series, II: Mathematics, Physics, and Chemistry; Kluwer: Dordrecht, The Netherlands, 2004; Vol. 172, pp 457–465.
- Zhu, Z.-T.; Musfeldt, J. L.; Kamaras, K.; Adams, G. B.; Page, J. B.; Kashevarova, L. S.; Rakhmanina, A. V.; Davydov, V. A. *Phys. Rev. B* **2002**, *65*, 085413.
- Zhu, Z.-T.; Musfeldt, J. L.; Kamaras, K.; Adams, G. B.; Page, J. B.; Kashevarova, L. S.; Rakhmanina, A. V.; Davydov, V. A. *Phys. Rev. B* **2003**, *67*, 045409.
- Popov, A. A.; Senyavin, V. M.; Granovskii, A. A. *Chem. Phys. Lett.* **2004**, *383*, 149–155.
- Popov, A. A.; Goryunkov, A. A.; Goldt, I. V.; Kareev, I. E.; Kuvychnko, I. V.; Hunnius, W. D.; Seppelt, K.; Strauss, S. H.; Boltalina, O. V. *J. Phys. Chem. A* **2004**, *108*, 11449–11456.
- Kuvychnko, I. V.; Streletskii, A. V.; Popov, A. A.; Kotsiris, S. G.; Drewello, T.; Strauss, S. H.; Boltalina, O. V. *Chem. Eur. J.* **2005**, *11*, 5426–5436.
- Popov, A. A.; Senyavin, V. M.; Troyanov, S. I. *J. Phys. Chem. A*, in press.
- Laikov, D. N. *Chem. Phys. Lett.* **1997**, *281*, 151–156.
- Perdew, J. P.; Burke, K.; Ernzerhof, M. *Phys. Rev. Lett.* **1996**, *77* (18), 3865–3868.
- Popov, A. A.; Senyavin, V. M.; Granovsky, A. A. *Fullerenes, Nanotubes, Carbon Nanostruct.* **2004**, *12*, 305–310.
- Baker, J.; Jarzecki, A. A.; Pulay, P. *J. Phys. Chem. A* **1998**, *102*, 1412–1424, and references therein.
- Rau, J. V.; Nunziante Cesaro, S.; Boltalina, O. V.; Agafonov V.; Popov, A. A.; Sidorov, L. N. *Vib. Spectrosc.* **2004**, *34*, 137–147.
- Bagryantsev, V. F.; Zapol'skii, A. S.; Boltalina, O. V.; Galeva, N. A.; Sidorov, L. N. *Dokl. Akad. Nauk* **1997**, *357*, 487–489.
- Granovsky, A. A. PC GAMESS, 2006. URL: <http://classic-chem.msu.su/gran/gamess/index.html>.
- Schmidt, M. W.; Baldrige, K. K.; Boatz, J. A.; Elbert, S. T.; Gordon, M. S.; Jensen, J. H.; Koseki, S.; Matsunaga, N.; Nguyen, K. A.; Su, S. J.; Windus, T. L.; Dupuis, M.; Montgomery, J. A. *J. Comput. Chem.* **1993**, *14*, 1347–1363.
- Yagola, A. G.; Kochikov, I. V.; Kuramshina, G. M.; Pentin, Y. A. *Inverse Problems of Vibrational Spectroscopy*; VSP, Zeist, The Netherlands, 1999.
- Boltalina, O. V.; Street, J. M.; Taylor, R. *J. Chem. Soc., Perkin Trans. 2* **1998**, 649–654.
- Boltalina, O. V.; Buhl, M.; Khong, A.; Saunders, M.; Street, J. M.; Taylor, R. *J. Chem. Soc., Perkin Trans. 2* **1999**, 1475–1479.
- Clare, B. W.; Kepert, D. L. *J. Mol. Struct. (THEOCHEM)* **1999**, *466*, 177–186.
- Clare, B. W.; Kepert, D. L. *J. Mol. Struct. (THEOCHEM)* **2002**, *589–590*, 195–207.
- Nossal, J.; Saini, R. K.; Sadana, A. K.; Bettinger, H. F.; Alemany, L. B.; Scuseria, G. E.; Billups, W. E.; Saunders, M.; Khong, A.; Weisemann, R. *J. Am. Chem. Soc.* **2001**, *123*, 8482–8495.
- Gakh, A. A.; Romanovich, A. Y.; Bax, A. *J. Am. Chem. Soc.* **2003**, *125*, 7902–7906.

- (52) Darwish, A. D.; Avent, A. G.; Taylor, R.; Walton, D. R. M. *J. Chem. Soc., Perkin Trans. 2* **1996**, 2051–2054.
- (53) Neretin, I. S.; Lyssenko, K. A.; Antipin, M. Y.; Slovokhotov, Y. L.; Boltalina, O. V.; Troshin, P. A.; Lukonin, A. Y.; Sidorov, L. N.; Taylor, R. *Angew. Chem., Int. Ed.* **2000**, *39*, 3273–3276.
- (54) Troyanov, S. I.; Shustova, N. B.; Popov, A. A.; Sidorov, L. N.; Kemnitz, E. *Angew. Chem., Int. Ed.* **2005**, *44*, 432–435.
- (55) Hitchcock, P. B.; Avent, A. G.; Martsinovich, N.; Troshin, P. A.; Taylor, R. *Chem. Commun. (Cambridge)* **2005**, 75–77.
- (56) Troshin, P. A.; Lyubovskaya, R. N.; Ioffe, I. N.; Shustova, N. B.; Kemnitz, E.; Troyanov, S. I. *Angew. Chem., Int. Ed.* **2005**, *44*, 234–237.
- (57) Troyanov, S. I.; Shustova, N. B.; Ioffe, I. N.; Turnbull, A. P.; Kemnitz, E. *Chem. Commun. (Cambridge)* **2005**, 72–74.
- (58) Goryunkov, A. A.; Markov, V. Y.; Ioffe, I. N.; Bolskar, R. D.; Diener, M. D.; Kuvychko, I. V.; Strauss, S. H.; Boltalina, O. V. *Angew. Chem., Int. Ed.* **2004**, *43*, 997–1000.
- (59) Troyanov, S. I.; Kemnitz, E. *Eur. J. Org. Chem.* **2003**, 3916–3919.
- (60) Darwish, A. D.; Martsinovich, N.; Street, J. M.; Taylor, R. *Chem. Eur. J.* **2005**, *11*, 5377–5380.
- (61) Cioslowski, J.; Rao, N.; Szarecka, A.; Pernal, K. *Mol. Phys.* **2001**, *99*, 1229–1232.
- (62) Boltalina, O. V.; Holloway, J. H.; Hope, E. G.; Street, J. M.; Taylor, R. *J. Chem. Soc., Perkin Trans. 2* **1998**, 1845–1850.
- (63) Street, J. M.; Clare, B. W.; Kepert, D. L.; Taylor, R. *J. Phys. Chem. B* **2004**, *108*, 19228–19232.
- (64) Avent, A. G.; Taylor, R. *Chem. Commun. (Cambridge)* **2002**, 2726–2727.
- (65) Computed spectra of the C_1 isomer are almost identical to that of $C_3-C_{60}F_{36}$ (see Supporting Information for the computed spectra of the individual isomers). With respect to this, and because the C_1 isomer constitutes less than 30% of the sample, analysis of the experimental data presented here is based on the computed spectra of the C_3 isomer alone.